Journal of Neuroscience Research 76:141–154 (2004)

Subcutaneous Tri-Block Copolymer Produces Recovery From Spinal Cord Injury

Richard B. Borgens,[1] Debbie Bohnert,[1] Brad Duerstock,[1] Daniel Spomar,[3] and Raphael C. Lee[2]

[1]Center for Paralysis Research, School of Veterinary Medicine, Purdue University, West Lafayette, Indiana
[2]Department of Surgery, Molecular Medicine, and Organismal Biology and Anatomy, The University of Chicago, Chicago, Illinois
[3]Division of Neurosurgery, Wishard Memorial Hospital, Indiana University Medical Center, Indianapolis

We have studied the ability of nonionic detergents and hydrophilic polymers to seal permeabilized membranes of damaged cells, rescuing them from progressive dissolution, degeneration, and death. We report that a single subcutaneous injection of the tri-block copolymer, Poloxamer 188 (P188) 6 hr after a severe compression of the adult guinea pig spinal cord is able to: (1) preserve the anatomic integrity of the cord; (2) produce a rapid recovery of nerve impulse conduction through the lesion; and (3) produce a behavioral recovery of a spinal cord dependent long tract spinal cord reflex. These observations stood out against a control group in blinded evaluation. Conduction through the lesion was monitored by stimulating the tibial nerve of the hind limb, and measuring the arrival of evoked potentials at the contralateral sensory cortex of the brain (somatosensory evoked potentials; SSEP). Behavioral recovery was determined by a return of sensitivity of formerly areflexic receptive fields of the cutaneous trunchi muscle (CTM) reflex. This contraction of back skin in response to tactile stimulation is totally dependent on the integrity of an identified bilateral column of ascending long tract axons. A statistically significant recovery of both SSEP conduction through the lesion and the CTM reflex occurred in P188-treated animals compared to vehicle-treated controls. Quantitative 3D computer reconstruction of the lesioned vertebral segment of spinal cord revealed a statistically significant sparing of spinal cord parenchyma and a significant reduction in cavitation of the spinal cord compared to control animals We determined that the proportion of P188-treated animals that recovered evoked potentials were nearly identical to that produced by a subcutaneous injection of polyethylene glycol (PEG). In contrast, P188 was not as effective as PEG in producing a recovery of CTM functioning. We discuss the likely differences in the mechanisms of action of these two polymers, and the possibilities inherent in a combined treatment.

Key words: spinal cord; neurotrauma; copolymer; P188; polyethylene glycol

For over two decades, the use of monoclonal antibodies as a means to label specific cells and their molecular components has revolutionized basic biological research. A development arising from membrane biophysics that was critical to the development of this new technology was the ability to fuse two different cells into one. In particular, the use of the hydrophilic polymer polyethylene glycol (PEG) was often used to fuse mouse myeloma cells with lymphocytes producing hybridomas, which allowed the development of immortal cell lines critical to production of monoclonal antibodies. We exploited this capability to fuse completely transected strips of adult guinea pig spinal cord. Strips of white matter were functionally reunited (fused) in vitro after a brief exposure to PEG (Shi et al., 1999). Electrophysiologic conduction across strips of spinal cord also reappeared rapidly in response to PEG after severe compression of the spinal cord (Shi and Borgens, 1999).

These in vitro studies of isolated spinal cords were followed by three investigations of the polymer's action as an experimental treatment for severe compression injury to the adult guinea pig. The first investigation evaluated a brief (2 min) topical application of an aqueous solution of PEG directly to the lesion after durotomy (Borgens and Shi, 2000). The second investigation evaluated a similar but 6–8-hr delayed application of PEG to the exposed spinal cord injury (Borgens et al., 2002), and the third assessed a subcutaneous injection of the polymer administered ~6 hr post-injury (Borgens and Bohnert, 2001). In every case a rapid (hours to days) and statistically significant recovery of electrophysiologic and behavioral function occurred in response to polymer administration.

Contract grant sponsor: National Institutes of Health; Contract grant number: 1 R01 NS 39288-01, 1 R01 NS/HD 39288-01A1, R01 GM61101, R01 GM64757.

*Correspondence to: Richard B. Borgens, PhD, Purdue University, 408 S. University Street, West Lafayette, IN 47907. E-mail: cpr@purdue.edu

Received 1 August 2003; Revised 30 October 2003; Accepted 8 December 2003

Published online 5 March 2004 in Wiley InterScience (www.interscience.wiley.com). DOI: 10.1002/jnr.20053

PEG, however, is not the only polymer that has shown the capability to interfere with progressive soft tissue destruction through an action in reversing or eliminating permeabilization of the cell membrane.

Another interesting family of polymers are the so-called tri-block copolymers, poloxamines and poloxamers. These nonionic detergents (in particular the Poloxamer P188) are also capable of sealing damaged cell membranes in various model systems (Lee et al., 1992; Padanlam et al., 1994; Merchant et al., 1998; Palmer et al., 1998; Marks et al., 2001; Maskarinec et al., 2002; reviewed by Borgens, 2001, 2003), but as well may provide long-term potent neuroprotection to neurons in culture (Marks et al., 2001). This latter action is likely due to the membrane-sealing capability of P188, and its ability to scavenge highly reactive oxygen species (ROS; free radicals). ROS concentrations are known to increase markedly in and near central nervous system (CNS) lesions unopposed by endogenous antioxidants whose production is reduced significantly after CNS injury (Young, 1993; Lewen et al., 2000). ROS are associated with the destruction of membranes by lipid peroxidation (LPO) in a positive feedback cycle, and contribute significantly to progressive destruction of CNS soft tissue after injury ("secondary injury," reviewed Young, 1993; Lewen et al., 2000; Borgens, 2003). Furthermore, P188 is believed to target the actual breach in the cell membrane through interaction of the hydrophobic poly-(polypropylene oxide) moiety of the polymer, which inserts directly into the exposed hydrophobic core of the "broken" membrane (Marks et al., 2001; Maskarinec et al., 2002).

We have tested and compared the ability of subcutaneously administered P188 to induce a behavioral and electrophysiologic recovery from spinal cord injury to that of subcutaneously administered PEG (Borgens and Bohnert, 2001) by testing its action using a similar protocol of study. We wished to exploit the free radical scavenging capability of P188 (PEG is not a free radical scavenger per se; Luo et al., 2002) and increase the level of specific targeting of the hemorrhagic injury after subcutaneous or intravenous injection (as does PEG, Borgens and Bohnert, 2001), but as well the actual breach in the plasma membrane (Marks et al., 2001). To accomplish this task, we have used the exact same electrophysiologic assay (SSEP conduction), anatomic evaluation (3D reconstruction of spinal cord lesions), and behavioral assay (the CTM reflex), as carried out in previous experiments using PEG (Borgens and Shi, 2000; Borgens and Bohnert, 2001; Borgens et al., 2002).

MATERIALS AND METHODS

Animal Surgical Procedures

Forty-three adult guinea pigs (ca. 300 g) were anesthetized with an intramuscular injection of 100 mg/kg ketamine HCl and 20 mg/kg xylazine. The spinal cord was exposed at vertebral levels T12–L1 by dorsal laminectomy. The spinal cord was crushed for a duration of 15 sec with special blunted forceps possessing a détente to produce a constant displacement injury (Blight, 1991; Moriarty et al., 1998; Borgens and Shi, 2000). To sedate animals for behavioral and physiologic testing, guinea pigs were injected with 0.1 cc sodium pentobarbital, 50 mg/ml. Two animals died immediately after surgery due to complications. The remaining 41 animals used in this two-pronged investigation were divided into a P188 dose-response study ($n = 20$) and a controlled comparative study of outcomes in spinal injured guinea pigs in response to subcutaneous (SubQ) administration of P188 ($n = 21$). All study animals were euthanized by deep anesthesia followed by perfusion/fixation.

In Vivo Somatosensory Evoked Potential Conduction

Functional deficits produced by spinal cord injury (SCI) are caused largely by the loss of nerve impulse conduction through mechanically damaged tracts of nerve fibers in spinal cord white matter (Blight, 1991; Follis et al., 1996). We thus evaluate the loss and recovery of electrophysiologic conduction through the spinal cord injury by evoked potential techniques (somatosensory evoked potential testing; SSEP). Stimulation of the tibial nerve of the hind limb produces ascending volleys of nerve impulses recorded at the contralateral sensory cortex of the brain. These SSEPs represent multisynapse afferent conduction through ascending long tract sensory columns and are immediately abolished by compression of the spinal cord between the site of stimulation and recording. Each complete electrical record was comprised of separate trains of 200 stimulations ($<$2 mA square wave, 200 μsec duration at 3 Hz). Three to four sets of these recordings were made at each measurement period and then averaged to produce the single waveform presented in the results.

As a control procedure, the median nerve of the forelimb (unaffected by the spinal cord injury at the midthoracic level) was stimulated. This control stimulation regimen was carried out in every circumstance where a failure to record evoked potentials at the cortex occurred in response to hind limb tibial nerve stimulation to eliminate the possibility these conduction failures were false negatives. SSEP recording and averaging was carried out with a Nihon Kohden Neuropak 4 stimulator/recorder and a PowerMac G3 computer. Typical examples of SSEP recordings, as well as median nerve control procedures are provided below.

Computation of the area beneath the early arriving SSEP peak (P1) was accomplished by scribing a reference line through the recording baseline (beneath the base of the peak), and determining the unit area contained within it as pixels using IPLab software (Scanalytics, Fairfax, VA). These measurements were made without knowledge of the experimental treatment (by D.B.). The peak areas were normalized by dividing the area of the post-injury SSEP recording by the initial area of the pre-injury recording. This normalized mean area under the curve would approach unity (1.0) if 100% of single nerve fibers contributing to the evoked potential were once again recruited into conduction subsequent to the injury.

In Vivo Conduction Response to Different P188 Dosages

To evaluate the dose response to P188, 20 guinea pigs (250–400 g) were injected subcutaneously beneath the skin on the back of the neck with different concentrations of P188. The

guinea pigs were divided into three groups: Group I received 150 mg/kg P188 ($n = 7$), Group II received 15 mg/kg P188 ($n = 7$), and Group III received 1.5 mg/kg P188 ($n = 6$). Each guinea pig received this subcutaneous injection 30 min after the spinal cord was crushed. Somatosensory evoked potential measurements were recorded (see above) before spinal cord injury, at 15, 30, and then at 30-min intervals up to 5 hr after P188 injection. For the purposes of comparison of proportions, an animal was considered to have recovered the SSEP if a reproducible early arriving peak (P1) could be recorded in a minimum of 7 of 11 measurements taken at each of the various time intervals. The proportions of animals that recovered in each group were then compared using Fisher's exact two-tailed test. The investigator (D.S.) was also unaware of the animal's experimental status during recording and evaluation of SSEPs throughout the entire dose-response evaluation.

Behavioral Recovery Testing

As an index of behavioral recovery, we evaluated a spinal cord-dependent contraction of back skin in animals, the cutaneus trunchi muscle reflex (CTM) (Blight et al., 1990; Borgens, 1992; Fig. 1). The loss of CTM behavior after injury to the spinal cord was observed as a region of back skin that no longer responded by muscular contraction to local tactile stimulation (Borgens et al., 1987; Blight et al., 1990; Borgens et al., 1990; Borgens, 1992). This areflexia does not recover for the life of the animal if the relevant (and identified) ascending CTM tract is severed within the ventral funiculus. After a severe bilateral crush injury of the midthoracic spinal cord (such as used here), a bilateral region of areflexia of back skin is produced that shows very limited ability to spontaneously recover. We estimate <15% rate of overall recovery in untreated animals based on over a decade of experience using this reflex as an index of white matter integrity. Complete details of the anatomically identified circuit, its physiology, behavioral loss and monitoring, and other testing of the CTM as a spinal cord injury model can be found in previous reports (Blight et al., 1990; Borgens et al., 1990; Borgens et al., 2002; Fig. 1).

P188 Treatment and Behavioral, Physiologic, and Anatomic Evaluation

The comparative study of electrophysiologic, behavioral, and anatomic, outcome from subcutaneous P188 injection after SCI used a total of 21 animals. The P188-treated group ($n = 11$) was compared to a vehicle-treated group ($n = 10$). For these studies, we suspended 100 mg/kg P188 (35% w/w in sterile lactated ringers (SLR)) in a citrate buffer. Approximately 6 hr after the spinal cord injury, 1 cc of P188 was injected subcutaneously beneath the skin of the neck in 11 spinal-injured guinea pigs using a 22-gauge needle. Ten spinal injured guinea pigs in the vehicle-treated control group received a single injection of

COLOR

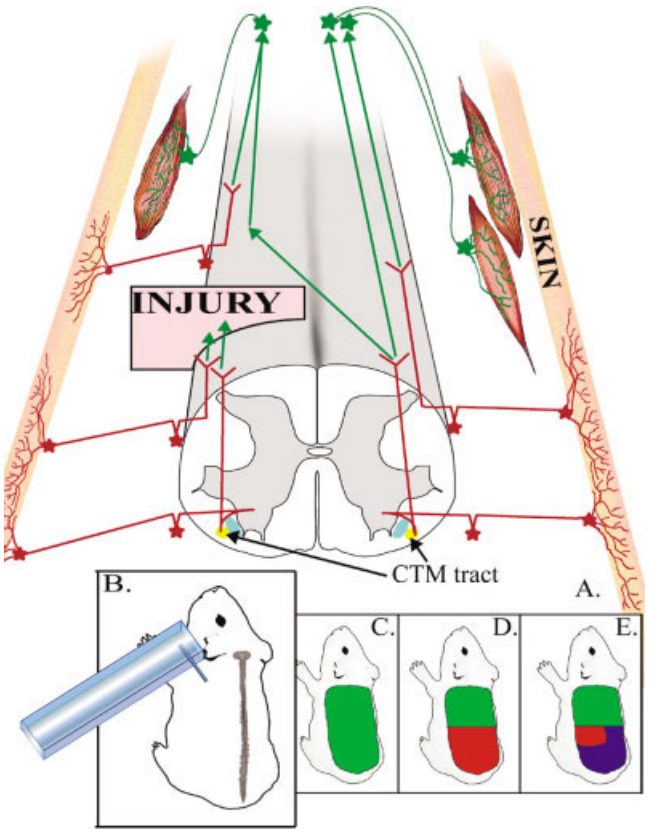

Fig. 1. CTM reflex circuit and behavioral evaluation. **A:** Elements of the CTM neural circuit, on the right side the intact circuit, on the left side, an injury to only that side of the spinal cord. On the right, dorsal root nociceptive reflex afferents (in red) project into the spinal cord from the back skin. The long tract CTM column (first order in red, second order in green) projects up the cord to a pool of motor neurons (green) in the thoraco/cervical region. This bilateral column (CTM tract, light yellow) is located in the medial/lateral portion of the spinal cord in the ventral funiculus, just lateral to the spinothalamic tract (light blue). Although there is evidence of contralateral projections arising from climbing afferents, there is no contralateral communication between left and right CTM motor neurons. Motor axons leave the spinal cord at the brachial plexus, and project to the cutaneous trunchi muscle of the skin via the lateral thoracic branch of the plexus. To explain the response to injury, we show that an injury to the left side of the spinal cord eliminates CTM conduction from below the lesion, whereas the receptive fields above the lesion and on the contralateral side are intact. Although we have utilized hemisection techniques, the cord was compressed equally on both sides eliminating all CTM reflex activity below the level of the lesion. **B:** A normal intact pig is shown as is a drawing of the monofilament probe used to stimulate the receptive fields of the back skin by light touch. **C:**) Intact receptive field is shown in green. Stimulation within the green area produced CTM skin contraction, whereas outside of the area did not. **D:** Region of areflexia is shown in red, secondary to an approximately midthoracic bilateral spinal cord injury. Probing within this region did not produce CTM contractions, whereas stimulation within the green (intact) region did. **E:** Blue region depicts an area of recovered CTM sensitivity. Probing within it elicits CTM contractions whereas probing outside, in the remaining region of areflexia (red), does not. In actual practice, the guinea pig has a matrix of dots tattooed on the back skin, and the entire process of probing the back skin to reveal CTM responsiveness, or the lack of it, is videotaped from above for computer graphic reconstruction. The movement of the dots as the skin moves allows a more sophisticated analysis of CTM movements if required (although not carried out here) (Borgens et al., 2002).

the vehicle (SLR). Only one subcutaneous injection per animal was made. CTM testing and SSEP recordings were carried out on all 21 animals before spinal cord injury, 1 day, 1 week, 3 weeks, and 6 weeks post-injury. The investigator (D.B.) carrying out surgery was kept unaware of the experimental group to which each coded animal would be randomly assigned. Furthermore, the syringes containing either the polymer or control solution were also coded so that blinding would be uncompromised throughout this investigation.

Histologic Preparation

The segments of spinal cord containing the lesion site (ca. >1 vertebral segment; ~1 cm in length) were removed by dissection 6 weeks after experimental injury. Every spinal cord segment was dehydrated in ascending concentrations of alcohol followed by xylene permitting infiltration and embedding in Paraplast (paraffin) by conventional methods. Each spinal cord segment was completely sectioned in 15-μm thick horizontally/longitudinally sections by a rotary microtome. The tissue sections were affixed to microscope slides that had been dipped previously in a 0.5% gelatin solution to enhance section adhesion. Paraffin was separated from slides, first by treatment in a 60%C oven for 1 hr, and then completely removed after immersion in 100% xylene for 1 hr. Rehydration of sections was conventionally carried out by immersing the tissues in descending concentrations of alcohol to distilled water. The sections were stained with Holme's silver stain to label the intact white and gray matter and counterstained with neutral red to reveal necrosis at the injury site. Cysts were easily visible due to the absence of stained tissue.

Video Capturing and Registration of Serial Sections

An Olympus Van Ox Universal (Optical Analysis, Indianapolis, IN) microscope mounted with an Optronics DEI-750 (Goleta, CA) color video camera displayed the histological sections on an adjacent computer monitor and Intel dual Pentium (Santa Clara, CA) computer using ImagePro Express (Media Cybernetics, Silver Springs, MD) to digitally capture their images. This software was used to register serial histologic images by optimally aligning the microscope stage so that successive histologic sections would compare to the transparent or "ghosted" image of the prior captured section. Boundaries of the spinal cord, cysts, and injury site were used for effective registration. The data sets of captured histologic images were then managed and three-dimensionally reconstructed on a Silicon Graphics Indigo computer (Mountain View, CA).

3D Reconstruction

In our technique, 3D reconstruction is a perceptive method that allows every histologic section in a segment of spinal cord to be visualized at one time. This technique grants a more comprehensive evaluation of spinal tissue than using and carrying out morphometric analysis on only a select few histologic sections within the data set (Duerstock et al., 2000). Note: all retrieved histologic sections obtained from the spinal segments were used during 3D reconstruction to ensure precise reproduction of spinal cord tissue and accuracy of measurements queried from them. When the microtome advanced into and out of the tissue, a few of the most dorsal and ventral sections were unusable or not retrieved. Figure 2 shows a typical 3D reconstruction of an uninjured segment of spinal cord. Note the minor loss of the most dorsal and ventral histologic sections flattens the appearance of the reconstructed spinal segment at the anterior/posterior margin. Good condition of serial histologic sections is thus important for effective registration and reconstruction of the entire data set. For this reason, 11 of the highest quality spinal cord data sets were chosen for 3D reconstruction (five control and six P188 application).

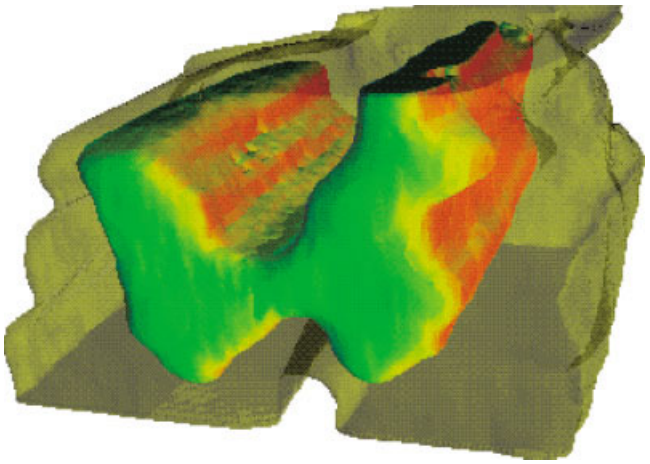

Fig. 2. Three dimensional reconstruction of an uninjured spinal cord segment. Three dimensional reconstruction of serial histologic sections was carried out using a novel isocontouring algorithm. Approximately 50 horizontal/longitudinal were used to produce this 3D image of a normal spinal cord segment. The dorsal posterior surface of the segment faces the top of the page. The isocontouring program automatically created isocontours around distinguishing features of interest, such as the familiar morphology of the gray matter (green and red) and the outer white matter tracts, shown in transparent gold. The volume and surface area of isocontours are quantified without user intervention. Every histologic section was used to produce this 3D reconstruction and those of the vehicle-treated and P188-treated spinal cord injuries, except those lost at the most dorsal and ventral portions of the cord when the microtome blade advances into the tissue and out of it. The loss of these small portions of tissue gives the reconstructed image a flattened appearance at the dorsal (posterior) and ventral (anterior) surfaces.

3D reconstruction was accomplished using the isocontouring algorithm (described in Bajaj et al., 1997). Isocontouring is a novel 3D reconstruction algorithm that uses pixel intensity differences within the component histologic images to produce 3D surfaces around biologic features of interest. The volume and surface area can also be computed automatically from the 3D isocontoured surfaces of reconstructed tissues (and objects imbedded within the tissues) for quantitative evaluation (Duerstock et al., 2000). Figure 2 is an example of 3D reconstruction by the isocontouring method using serial histologic sections from a normal spinal segment.

The investigator (B.D.) was blinded to the identity of experimental and control spinal cord injuries during all phases of 3D reconstruction, including capture of individual images comprising the histologic data sets, 3D imaging, and subsequent

quantitative interrogation. The identity code of the subjects was broken only after 3D reconstructions were completed, structures of interest were quantified, and the quantitative data was organized.

Post-Injury 3D Morphometry

The healthy, intact spinal cord parenchyma, lesioned tissue, and cysts in segments of P188-treated and vehicle-treated spinal cords (ca. 4.2 mm long) were quantified precisely from their 3D reconstructions. Holme's silver stain served as an effective label for the intact regions of white matter, which appeared dark red to purple at low magnification due to staining of axons against a neutral red background stain. The lesion appeared light red due to the absence of silver impregnated neurons.

Volume and surface area measurements of pathologic features of interest from the 3D reconstructions were normalized by dividing each metric by the volume or surface area of that spinal cord segment and multiplying by 100. This resulted in a percentage of total volume or surface area of an anatomic feature of interest relative to the varying size of the spinal cord segment containing it. The intact parenchyma could be measured directly from the 3D reconstructions, whereas the volume and surface area of cysts were calculated by subtracting the healthy and necrotic tissue from the size of the total spinal cord segment. The volume and surface area of the lesion was calculated by subtracting the measurements of undamaged spinal cord parenchyma from the total nervous tissue without cysts (Duerstock and Borgens, 2002). A negative measurement therefore would result sometimes if the surface area of the undamaged parenchyma was greater than the surface area of the total spinal cord tissue.

Statistical Evaluation

Statistical computations were carried out using InStat software (GraphPad, San Diego, CA). Comparison of the proportions of animals in each group tested for evoked potentials was carried out using Fisher's exact test (two-tailed) and a comparison of means with Mann-Whitney nonparametric two-tailed test. Normalized measurements from 3D reconstructions of control and experimental groups were compared using unpaired, two-tailed, Student's *t*-test.

RESULTS

Nerve Conduction Evaluation at Differing Dosages of P188

Clearly, the high dosage group (~150 mg/kg) outperformed the other two dilutions (15 and 1.5 mg/ kg) when induction of SSEPs over a 15 min to 5-hr period were compared. Six of seven animals in the high dosage group recovered reproducible SSEPs over this time, compared to only two of seven in the 15 mg/kg group ($P = 0.03$, Fisher's exact test, two-tailed) and similarly, one of six animals in the 1.5 mg/kg group ($P = 0.03$; Fisher's exact test, two-tailed; Fig. 3). When the integrated amplitude and duration of the early arriving peak was compared between groups (at time points where at least two of them possessed a measurable SSEP), the normalized mean of the high dosage group was consistently, statistically, significantly, larger than either one of the two comparator groups without exception (high dose vs. low dose at 1 hr, $P = 0.03$; 2 hr, $P = 0.005$; high dose vs. intermediate dose at 2 hr, $P = 0.0002$). At all other time points intermediate and low concentrations did not produce a measurable SSEP at the cortex after stimulation of the tibial nerve with which to compare. When P1 data for all measurement periods were compared, the high dosage group was consistently significantly greater than the comparator groups (high vs. intermediate dose, $P = 0.0003$; and high vs. low dose, $P < 0.0001$). Table I and II summarize these data, and Figure 3 provides a comparison of typical electrical records taken during this study.

Comparative Study of Outcomes: Recovery of Conduction Through the Injured Spinal Cord

P188 treatment resulted in a significantly greater proportion of animals recovering SSEP conduction after experimental spinal injury than did vehicle-treated animals at all time periods (1 day, 1 week, 3 weeks, and 6 weeks). One day after injury, 10 of 11 P188-treated animals recovered SSEP conduction, compared to 3 of 10 vehicle-treated animals ($P = 0.0075$, Fisher's exact test). By 1 week post-injury, the proportions of P188-treated animals that recovered an SSEP had not changed (10/11). One animal of the control group, however, could no longer be stimulated to produce an SSEP, enhancing the statistical difference between the groups (proportions: 2/10, $P = 0.0019$, Fisher's exact test). This proportion did not change at 3 weeks. By 6 weeks post-injury, however, another recovered animal in the vehicle-treated control group could no longer be stimulated to produce a measurable SSEP (proportion: 1/10 recovered: $P = 0.0003$, Fisher's exact test). To summarize, throughout the 6-week time course of the study, an average of ~91% of P188-treated animals recovered SSEP nerve conduction compared to ~10% of vehicle-treated animals (Fig. 3; Table II).

The area under the early arriving SSEP waveform (P1) was determined for 10 of 11 P188-treated animals that recovered conduction through the lesion at 30 days post-injury (the time when recovering SSEP amplitudes were maximal).

Before spinal cord injury, the average area in pixels for P1 for the 10 records was 8076.7 ± 371.1; 6 weeks after injury it was 11381.0 ± 2610.1. This difference in the means was not statistically different ($P = 0.16$, Mann-Whitney, two-tailed test). This reveals that the shape of the early arriving waveform (that is, integrated amplitude and duration) was not different from that measured before injury. Given the sensitivity and normal variation in these types of recordings we did not consider any difference in latency ≤4 msec slower or faster than that recorded before SCI to be abnormal. Using this as an index, seven of ten 1-month records showed an extended latency, the longest increase from the stimulus to the initiation of the evoked potential being 14 msec.

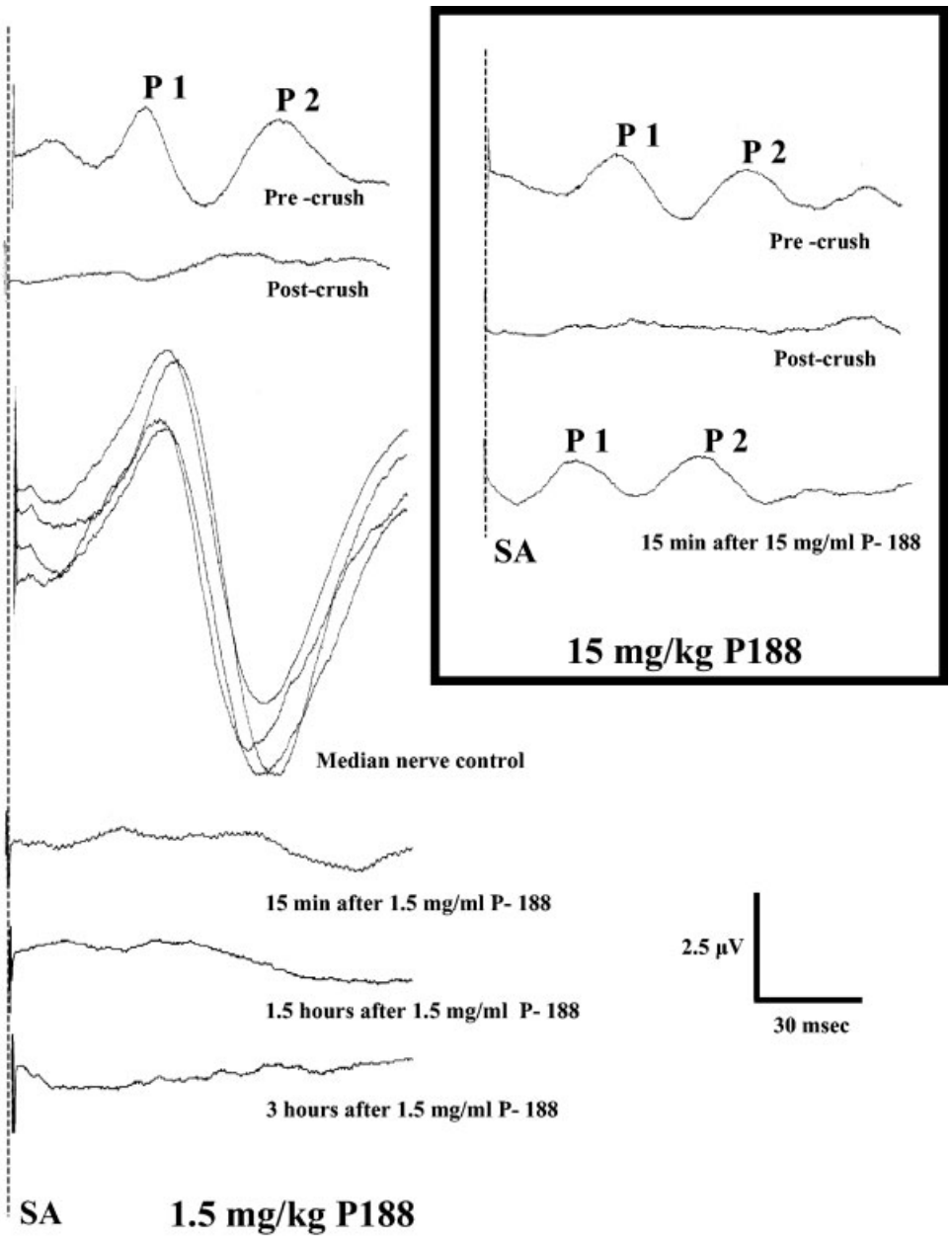

Fig. 3. Electrophysiologic responses to intravenous P188 at two concentrations. At the top left, a typical SSEP is shown as recorded from normal animals. This single waveform is an average of evoked potentials resulting from three to four 200 stimulation trains. An early and late arriving peak (P1 and P2) is also typical of the intact animal. Immediately after a constant displacement crush injury to the midthoracic spinal cord, the SSEPs recorded at the sensory cortex have been eliminated (post-crush record). The three large amplitude waveforms (not averaged) are three highly reproducible trains of stimulation of the median nerve of the forelimb in this same animal after SCI. This control recording is produced by stimulating a neural circuit above the level of the lesion, and demonstrates that the lack of evoked potential(s) after stimulation of the tibial nerve constitutes a failure of conduction through the SCI. A low dose of P188 (1.5 mg/kg) was administered intravenously via the jugular vein while recordings were continued in this animal. Three signal-averaged waveforms (of 11 time points) reveal the lack of response. Recovery of a reproducible SSEP could not be elicited for 5 hr after the injection at which time recordings were discontinued. The inset shows the progress of another animal given a high dose of P188 (15 mg/kg). Note the very rapid recovery of the early and late arriving peaks by 15 min after injection. This recovered evoked potential was consistently reproducible throughout the 5 hr of recording. This particular animal revealed a slightly reduced latency in P1 and P2 compared to normal. This is not typical of the population, where SSEP latency was usually longer during the early phase of SSEP recovery. SA, stimulus artifact; the scale is for all electrical records shown.

TABLE I. Cutaneous Trunchi Muscle Response to P188

Group	*n*	% Loss[a]	*P*[b]	Recovered (*n*)[c]	*P*[b]	% Recovered[d]
P188	11	47.0 ± 2.6	0.13	5	0.03	40.8 ± 5.3
Control	10	41.3 ± 3.3		0		

[a]The percentage of the total cutaneous trunchi muscle (CTM) receptive field that was lost after spinal injury (mean ± SE).
[b]Statistical difference between the two groups compared with Fisher's exact test, two- tailed.
[c]The number of animals that recovered any portion of the CTM by 1 month post injury.
[d]The percentage of the area of areflexia that recovered after P188 treatment (mean ± SE).

TABLE II. Somatosensory Evoked Potential Response to P188

					Amplitude/duration[d]		
Group	*n*	Loss[a]	Recovered[b]	*P*[c]	Before injury	After injury	*P*[c]
P188	11	11	10	0.002	8,076.7 ± 371.1	11,381 ± 2,610.1	0.16
Control	10	10	2				

[a]The number of animals in which somatosensory evoked potential (SSEP) conduction was eliminated by the spinal cord injury.
[b]The number of animals that recovered SSEP conduction through the lesion by 1-month post injury.
[c]Statistical difference between the two groups compared with Fisher's exact test, two-tailed.
[d]Amplitude and duration of the SSEP: mean ± SE of the area under SSEP early-arriving Peak 1 counted as pixels before and after the spinal cord injury. This measurement effectively integrates the amplitude and duration of the waveform.

Comparative Study of Outcomes: Behavioral Recovery

A behavioral recovery of the CTM in response to P188 injection was observed within hours in a few animals. Before 24 hr had elapsed after subcutaneous injection, 3 of 11 polymer-treated animals had already recovered variable amounts of the areflexic CTM receptive field below the lesion whereas none of the control group had (this difference was not significant, however, given the small sample size; $P = 0.2$; Fisher's exact test, two-tailed). By the end of the week, 5 of 11 animals had recovered variable CTM functioning, whereas none of 10 vehicle-treated animals had ($P = 0.03$, Fisher's exact test, two-tailed). In fact, none of the control group showed evidence of CTM recovery throughout the 1-month observation period, whereas those P188-treated animals that had recovered CTM functioning at 1 week post injury maintained recovery at 1 month. A statistically significant recovery of this sensory-motor function was observed in this study (summarized in Table I, Fig. 4).

We also evaluated if the spinal cord injury produced an equivalent loss of CTM functioning in the P188-treated group compared to that in the control group. This was determined by dividing the area of the CTM loss by the area of the CTM receptive field before injury, giving a percent loss in this region of receptive fields . In the control group, the standardized compression of the cord resulted in an average loss of the CTM receptive field of 41%. In the P188-treated group, the SCI resulted in an average loss of 47%. This difference was not statistically significant ($P = 0.13$, Student's *t*-test, two-tailed); thus, the behavioral loss after SCI in both groups was equivalent. These data are summarized in Table III. Only P188-treated animals recovered a measurable area of the areflexic field; however, this was variable in its extent, ranging from 5–54% (mean = 40.8%; Table I, Fig. 4).

Comparative Study of Outcomes: 3D Anatomic Studies

Due to the severity of the crush injury, injured segments of spinal cord were compressed and stenotic (Fig. 5i). For every 3D reconstruction, the injury site was centrally located at the region where the spinal cord was most compressed during registration of the images. The bilateral indentation of the crush injury was evident in many of the 3D reconstructions (Fig. 5Bi). Typically, after a constant displacement injury a hemorrhagic lesion is produced, causing profound destruction of the central gray matter of the spinal cord and variable sparing of the circumferential white matter (Moriarty et al., 1998; Tuszynski et al., 1999; Duerstock and Borgens, 2002). The 3D reconstruction processes both imaged and quantified regions of destroyed gray matter, marginal areas of spared gray and white matter, and cysts. Figure 5A and 5B include insets of histologic sections from the lesion epicenter of vehicle-treated and P188-treated reconstructed spinal cord segments, respectively. These histologic photomicrographs show thin tracts of spared silver impregnated axons of the white matter, whereas more central columns and most gray matter were destroyed. The images (ii) in Figure 5 show regions of apparently normal parenchyma in control (vehicle-treated) and P188-treated spinal cords. This intact parenchyma in control segments was located mainly in the subpial region and was virtually

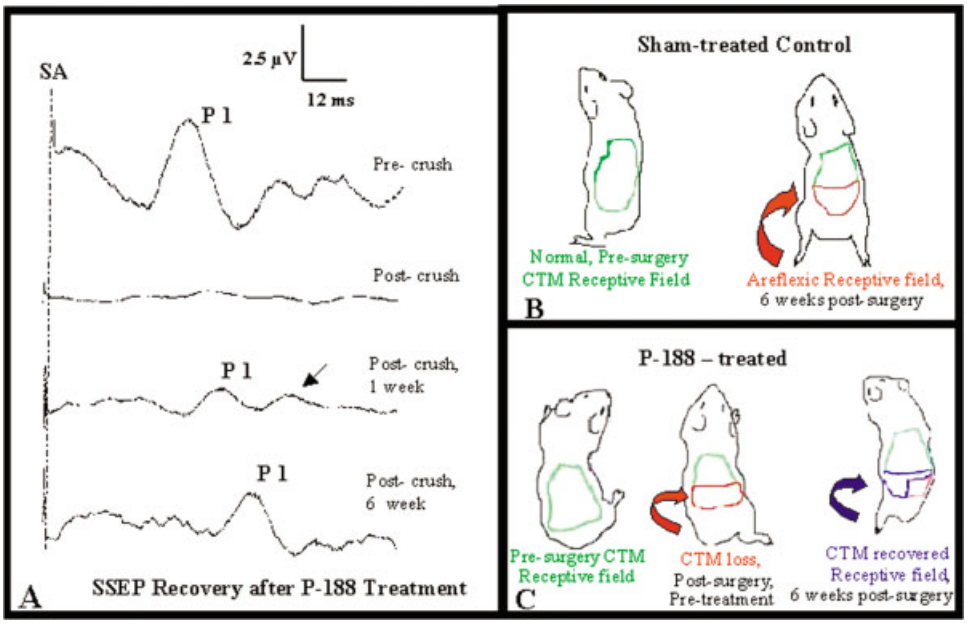

Fig. 4. P188-mediated recovery from SCI. **A:** Waveform at the top is the averaged signal of three trains of stimulations of the tibial nerve of the hind limb as recorded at the contralateral cortex in an intact guinea pig as described in the text and in Figure 3. A large early arriving evoked potential (EP; P1) is characteristic of SSEP recordings in normal animals, as are the late arriving, low magnitude EPs. A standardized compression of the cord eliminated SSEP conduction in this animal as in all animals for all previous studies in this series (Shi and Borgens, 2000; Borgens and Bohnert, 2001; Borgens et al., 2002). One week after a single subQ injection of P188, the early EP was consistently recorded, as was low amplitude, late arriving SSEPs (arrow). By 6 weeks, P1 had increased in amplitude significantly, but with increased latency. **B:** Normal CTM receptive field has been computer rendered from captured individual videotape frames of receptive field testing in one control animal. This particular animal did not recover any portion of the region of areflexia during ~6 weeks of observation. **C:** A similar CTM loss is shown, although by 6 weeks after P188 injection, approximately 58% of the formerly areflexic receptive field had recovered CTM sensitivity (the recovered receptive fields outlined in blue).

TABLE III. Comparison of PEG Recovery of Somatosensory Evoked Potentials and Cutaneous Trunchi Muscle Reflex★

Recovery	Experimental application	Animal	Number recovered/total[a]	Time after treatment[b]	*P*[c]
SSEP	Acute PEG[d]	C11	0/11	4 days	≤0.0003
		E14	13/14		
	Delay PEG[c]	C13	0/13	1 month	≤0.0001
		E15	15/15		
	SubQ PEG[f]	C10	0/10	1 month	≤0.0001
		E10	10/10		
CTM reflex	Acute PEG[d]	C11	0/11	4 days	≤0.0005
		E14	10/14		
	Delay PEG[c]	C13	3/13	1 month	≤0.0003
		E15	14/15		
	SubQ PEG[f]	C10	0/10	1 month	≤0.001
		E10	10/10		

★Comparison of cutaneous trunchi muscle (CTM) behavioral data and electrophysiologic measurement of ascending somatosensory evoked potentials (SSEP) conduction through the lesion in three published reports. Aqueous solutions of polyethylene glycol (PEG) were applied topically to the spinal cord lesion for 2 minutes in the first two experiments (acute and a 6–8 hour delay PEG). The third application was a single SubQ injection of PEG beneath the skin of the neck (1 cc of 30% PEG in sterile ringers; ≈mol. wt. 2,000 Da). This injection was made 6 hours after spinal cord injury.

[a]The total number of animals completing the experiment in C, control group; and E, the PEG-treated group.

[b]The time point at which animals received their last physiologic or behavioral examination and were sacrificed for anatomic study.

[c]Statistical evaluation was a test of proportions; Fisher's exact test, two-tailed.

[d]Report published in Borgens and Shi, 2000, FASEB.

[e]Report published in Borgens et al., 2002, J Exp Biol.

[f]Report published in Borgens and Bohnert, 2001, J Neurol Res.

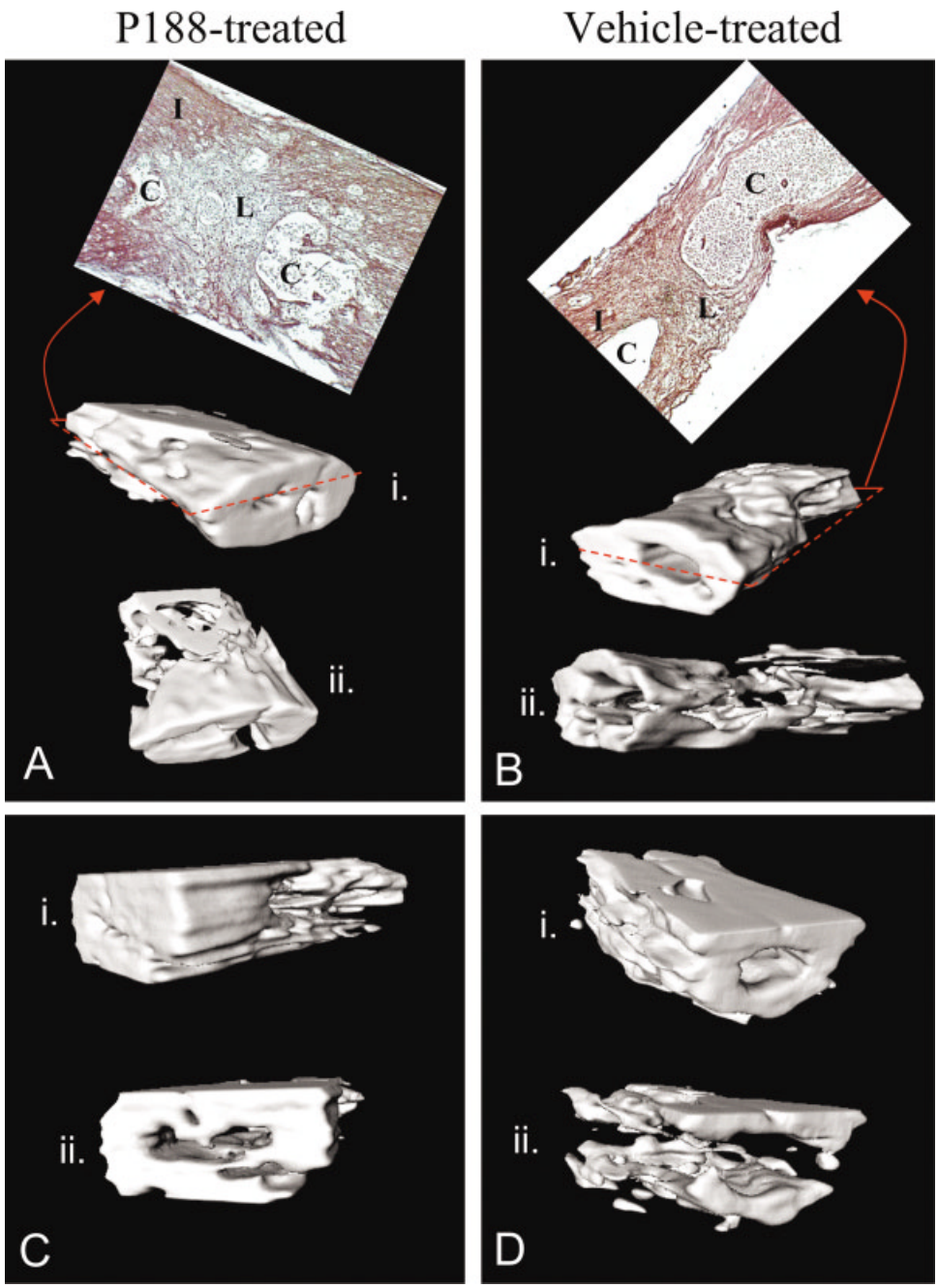

Fig. 5. Comparison of recovery of healthy parenchyma between P188 and vehicle-treated injuries. **A,C:** Three dimensional reconstructions of two P188-treated spinal segments. **B,D:** Three dimensional images of vehicle-treated spinal injured segments. In all frames, *i* shows severely injured segments reconstructed without cysts. Note the stenotic shape of the compressed spinal segments. The dorsal aspects of all 3D images are toward the top of the page. Pronounced cavitation of these injuries can be seen extending from the ends of many segments (Ai, Bi, and Di); **ii** shows 3D images of only the intact, healthy parenchyma (gray and white matter) slightly rotated in the horizontal plane from i. The greatest amount of tissue sparing occurred at the subpial rim of the cord with deterioration of the central gray matter. Insets of photomicrographs from the lesion epicenters of spinal segments in (A) and (B) are included (A,B top). These photomicrographs show one of the many histologic sections that composed the 3D reconstructions. I, dark red staining of intact neurons and axons; C, large cysts with the spinal segment; L, centralized lesion area devoid of silver impregnated neurons and nerve fibers. Cysts were greater in the untreated spinal cord injuries (Fig. 6). Each spinal segment is ~4.2 mm long.

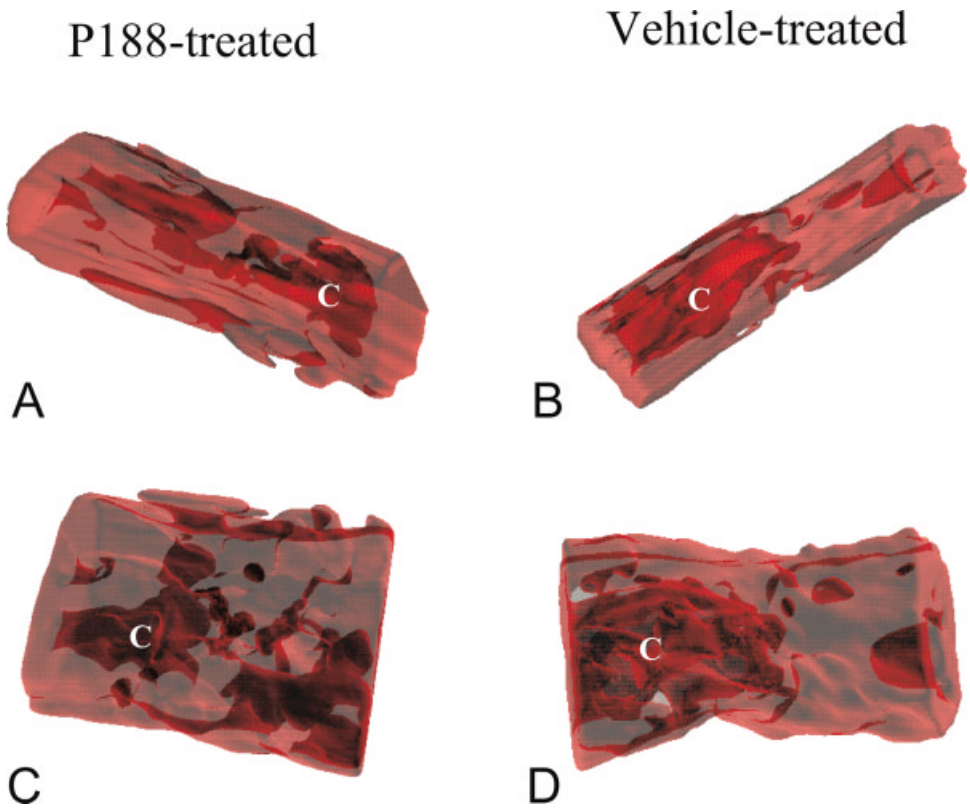

Fig. 6. Comparison of cyst formation between P188- and vehicle-treated spinal injuries. 3D reconstructions of injured spinal cord segments in Figure 5A,B were made transparent to better reveal their internal cysts. The dark red regions are cysts (labeled c). **A:** Lateral view of a P188-treated segment where the dorsal surface is at the top of the page and the rostral end is on the left. **C:** Same experimental spinal segment, rotated vertically 90°. Cysts are relatively small and dispersed throughout the injury site. **B,D:** Chronic cavitation of an untreated spinal cord segment. One large cyst consumed the caudal half of the spinal segment. B: Dorsal surface is at the top of the page showing a lateral view of the segment. B,D: Rostral end is on the right side. D: Rotated vertically 90° to reveal a dorsal view of the spinal segment. Typically, control cords exhibited larger, more localized cavities than those found in P188-treated spinal cords.

nonexistent at the lesion epicenter (Fig. 5Bii, Dii). Normal appearing parenchyma (both gray and white) was more abundant in P188-treated spinal segments than in control spinal cords (Fig. 5Aii, Cii). The amount of cavitation in these cords was the simplest pathologic feature to discriminate between the groups (Fig. 6). In the P188-treated spinal cord segments, cysts were smaller and dispersed more variably on either side of the central lesion (Fig. 6A,C). In the vehicle-treated spinal cords, cysts were larger and more localized within the spinal cord segment (Fig. 5, insets; Fig. 6B,D). Often cavitation was not confined within the field of view, extending beyond that particular segment of spinal cord (Fig. 5i). The area of scarification, devoid of silver impregnated nerve fibers, was located centrally at the region where the spinal cord was most compressed. In the vehicle-treated spinal cords, the lesion appeared less focal than in PEG-treated cords and tended to surround the cysts (Fig. 5, insets).

Volume measurements permitted whole-cord comparisons of the amount of spared and pathologic tissue in the spinal segment whereas measurements of surface area indicated the intricacy or complexity of structures such as the lesion. In Figure 7, the percentages of volume and surface area of healthy parenchyma, lesion tissue, and cysts in injured spinal segments were compared between vehicle-treated and P188-treated populations. The mean volume of normal appearing parenchyma after trauma in control spinal segments was 41.1% compared to 56.5% in P188-treated spinal cords (Fig. 7). Consequently, the amount of spared silver stained nerve fibers after P188 application was significantly greater in the experimental animals ($P = 0.0006$, Student's t-test). On average, 24.7% of the total volume of control spinal cord segments consisted of cysts compared to 14% in P188-treated spinal cords (Fig. 7). The volume of cavitation was significantly less in P188-treated animals than in the vehicle-treated animals ($P = 0.039$, Student's t-test). Surface area measurements suggested a more complex lesion site in vehicle-treated injuries (Fig. 7), however, quantitative comparison revealed there were no significant differences in any of the surface area measurements between vehicle-treated and P188-treated spinal cord injury structures ($P > 0.05$, Student's t-test).

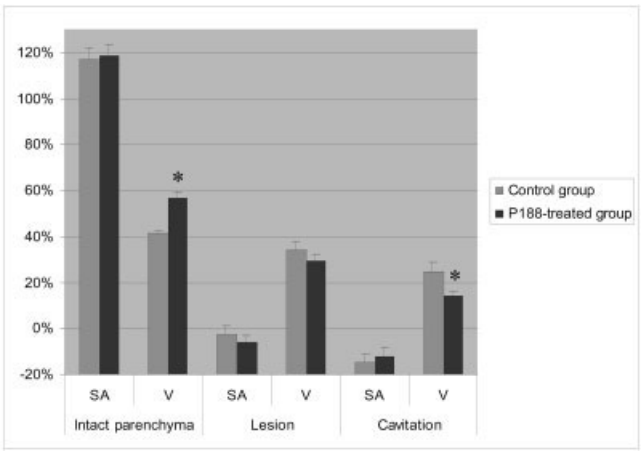

Fig. 7. Quantitative comparison of spatial measurements of spinal cord injury structures. The volume and surface area measurements of intact or healthy parenchyma, lesion, and cavitation are given as percentages of the whole injured spinal segment to normalize values for varying spinal cord diameters (length was constant at 4.2 mm). SA, surface area; V, volume. The volume of spared, healthy tissue was significantly greater in P188-treated subjects than in the control group. The total volume of cavitation was significantly less after P188 treatment compared to that in vehicle treatment. Surface area and lesion volume measurements were not significantly different. Error bars = SEM. $\star P < 0.05$, Student's *t*-test.

DISCUSSION

The use of tri-block copolymers in reversing membrane permeabilization in other injury and ischemia models were introduced earlier. We add to this emerging picture a beneficial usage of tri-block copolymers as an acute treatment for neurotrauma. In particular, we report that a single subcutaneous injection of P188 6 hr after a standardized compression injury to the adult guinea pig spinal cord produced these three major findings: (1) the recovery of SSEP conduction was enhanced by P188 treatment (<90% of the population) compared to an insignificant spontaneous recovery in the control group; (2) the midthoracic injury produced a similar area of areflexia in the CTM reflex in both groups, although a statistically significant recovery of these silent receptive fields occurred only in response to P188 treatment; and (3) 3D reconstruction of all serial histologic sections comprising the injured segments of spinal cord showed that P188 treatment reduced the amount of pathologic cavitation of the cords and was associated with an increased volume of intact parenchyma.

Tri-Block Copolymers Versus PEG: Comparison of Effects in SCI

Our studies of the possible beneficial response to the acute administration of polymers in SCI began with the use of PEG. We investigated varying types of administration, as well as the timing of the treatment in three separate studies. PEG consistently produced significant recovery of conduction through the lesion and CTM behavioral recovery compared to a vehicle-treated control group in each of these studies. These results are summarized in Table III. It is important to point out the three PEG investigations utilized identical methods of spinal cord compression, SSEP recording, CTM reflex evaluation as that employed in this investigation of P188. We compared the results of the delayed application of PEG to the spinal lesion after durotomy (Borgens et al., 2002) and the delayed subcutaneous administration of PEG (Borgens and Bohnert, 2001) to recoveries induced by subcutaneous injection of the Poloxamer. We compared the 3- and 6-week proportions of the latter to the 4-week data of the former. These data actually provided only two statistical comparisons of interest, given that the proportions of P188-treated guinea pigs that recovered SSEP conduction or CTM functioning did not change between the 3- and 6-week measurement periods. The results of these comparisons were interesting. First, there was no statistical difference in the frequency of SSEP recovery between either type of PEG application and the injection of P188 ($P = 0.4$, subcutaneous P188 vs. delayed topical PEG; and $P = 1.0$, subcutaneous P188 vs. subcutaneous PEG). Second, there was a significantly reduced frequency of recovery of the CTM reflex produced by P188 injection compared to PEG ($P = 0.02$, subcutaneous P188 vs. delayed topical PEG; and $P = 0.03$, subcutaneous P188 vs. subcutaneous PEG). It is useful to consider that the CTM reflex may likely be a more sensitive indicator of axonal survival in the spinal cord than of the recovery of SSEP conduction. The former is a completely identified neural circuit that possesses a minimal number of synapses between excitation of CTM receptive fields and their responsiveness to excitation (Blight et al., 1990). The recovery of evoked potentials, although a useful indicator of spinal cord integrity, can reemerge due to several factors. The data provided here seems consistent with the notion that PEG is likely to be more effective than P188 in the particular context of spinal cord injury. Third, such a difference in behavioral outcome was not entirely unexpected. When PEG is injected beneath the epineural sheath in the vicinity of a sciatic nerve injury, a significant recovery of target muscle physiology and force of contraction (measured in dynes) occurred (Donaldson et al., 2002). Intravenous PEG cannot produce a similar recovery of function in the sciatic nerve/gastrocnemius model, but P188 is able to do so (Altizer and Borgens, unpublished observations). It is thus likely the different mechanisms of action of the two polymers may become unmasked during use indifferent types of neurotrauma models. A short report suggested that intravenous P188 did not induce a recovery of function or anatomic preservation of spinal cord after aortic cross clamping, which produces an ischemic injury in rats (Follis et al., 1996). A very striking and rapid recovery of function indeed did occur in response to P188 injection in this study during the first few days post-injection ($P = 0.0001$). The claimed lack of effect was based on the fact that by 1

month, recoveries in control rats caught up with experimental ones. Given enough time post-injury, recovery of voluntary locomotion usually happens independent of the experimental treatment (Borgens, 2003). This is why motor skills in the extremities and crude measurements of sensation should not be used as indicators of white matter integrity in small animal models of spinal cord injury, and why we choose to use an alternate model that shows little to no spontaneous recovery: the CTM reflex (reviewed by Borgens, 2003). Furthermore, claims of a lack of effect on the anatomy of the ischemic lesion were not supported by either photomicrographs or complete quantitative data in this study (Follis et al., 1996).

Postulated Mechanisms of Action: P188 and PEG in SCI

As is typical of all physical trauma to tissue, mechanical injury is first manifested upon the cell membrane, whereas additional and progressive cell and tissue level pathology produce danger, perhaps catastrophic, for the organism. Animal tissues, however, possess reparative strategies for self-repair of the membrane. Cell, tissue, and organism levels of organization have evolved to interfere with or vitiate this cascade of injury, and the net result to the organism of the initial or primary insult is the balance between these two. Examples of repair strategies at the four main levels of organization include: (1) membranes have endogenous means of reassembly, repair, and sealing of breaches in response to insult; (2) cell hypertrophy and hyperplasia are means of restoring the volume or density of the cell mass; (3) scar tissue formation and epimorphic regeneration protect or restore the architecture of tissues; and (4) the immune reaction and the related inflammatory cascade can be considered an organismic response to injury. One might reasonably argue that the administration of polymers may replace or enhance these endogenous mechanisms of animal preservation/protection at several levels. There is incontrovertible evidence, however, to support a very active role of polymer mediation of injury at the level of the membrane and at the level of the inflammatory cascade.

Polymers Seal the Plasmalemma and Protect the Cell

Our original use of PEG was based upon its ability to fuse cell membranes. This capability was also exploited to restore the integrity of the membrane after compression injury. Damage to the processes of cells such as axons is believed to initiate a poorly regulated entry of Ca^{2+}, which in a positive feed back cycle further destabilizes the membrane (leading to gross ionic derangement), the associated destruction of the cytoskeleton, and even the initiation of apoptosis (reviewed by Borgens, 1982, 2003; Young, 1993). The exact molecular interaction of polymers with membrane irregularities, however, is not entirely understood (Lee and Lentz, 1997; Maskarinec et al., 2002).

Nevertheless, it is a clear fact that PEG and various Poloxamers can indeed seal membranes, although perhaps imperfectly at the outset. This has been demonstrated by significant reduction in the uptake of two extracellularly applied markers by injured axons (horseradish peroxidase and ethidium bromide; approximately <40 kDa and 400 Da, respectively) in response to PEG application (Shi and Borgens, 2000; Luo et al., 2002). Another excellent index of membrane breach is the loss of lactate dehydrogenase (LDH) from the cytoplasm into the extracellular space after cell injury (Koh and Choi, 1987). A brief exposure of PEG ($\sim$2 min) also significantly reduces LDH loss from axons after injury (Luo et al., 2002).

Application of P188 has also been shown to seal breaches in other types of cell membranes, restricting or eliminating transmembrane movement of intracellular markers. For example, P188 reduces the leakage of various markers in muscle cells in vitro (Lee et al., 1994; Merchant et al., 1998; Terry et al., 1999; Hannig et al., 2000; Maskarinec et al., 2002). Interestingly, as the P188 interaction allows restructuring of the membrane, the membrane surface pressure returns to normal, displacing the polymer and effectively ejecting it from the now-repaired membrane (Maskarinec et al., 2002).

P188, PEG, and the Inflammatory Cascade

After tissue injury, the inflammatory cascade usually produces collateral tissue damage in the course of its action. In the CNS, the collateral damage may outweigh the main benefit. This is likely true for the CNS, but clearly true for the reaction of the mammalian spinal cord to injury (reviewed by Borgens, 2003). Such secondary injury in spinal cord is exacerbated markedly by aberrant oxidative metabolism triggering the production of highly destructive reactive oxygen species (ROS; so-called free radicals). This is in concert with the closely related problem of upregulated lipid peroxidation of membrane components. These processes lead to toxic intermediates such as acrolein and hydrononeal, which further induce free radical production and more LPO in a positive self-reinforcing spiral. Normally in other tissues, ROS and LPO are held in check by several mechanisms such as the upregulation of endogenous antioxidants. In the spinal cord lesion, however, for reasons not entirely understood, the concentration of extracellular antioxidants plummets (see Borgens, 2003). As an aside, the use of glucocorticoid therapy for human clinical SCI was based on the notion that methylprednisilone would act as a potent free radical scavenger, helping to reduce the damaging consequences of ROS and LPO if administered within hours after spinal cord injury (Hall, 1992).

In an additional series of experiments, we have determined that PEG administration also reduces the concentration of free radicals in the spinal injury, but not as an antioxidant or scavenger, like ascorbic acid, superoxide dismutase, or P188. This reduction was evaluated by an assay based on reduction of the ROS-sensitive dye hydroethidine (Luo et al., 2002, after the method of Bindokas et al., 1996; and Chan et al., 1998). PEG application markedly reduces the concentrations of soluble LPO in cell-free extract of injured guinea pig spinal cord assayed by the

hydroperoxide method (Luo et al., 2002). PEG, however, does not reduce the concentration of stable free radicals in cell-free extract of lesioned guinea pig spinal cord revealed by the 1,1-Diphenyl-2-picrylhydrazl (DPPH) assay (after a method by Mellors and Tappel, 1996). PEG does not possess typical antioxidant properties at all compared to the comparator standards (superoxide dismutase and ascorbic acid) in these studies, although PEG still markedly reduced ROS. Competitive inhibition of the xanthine/xanthine oxidase reaction for reduction of cytochrome *c* is a specific probe for superoxide concentration (Quick et al., 2000). PEG at two different concentrations (5 and 50%) completely failed to inhibit cytochrome *c* reduction. Xanthine oxidase (XO) is a critical enzyme in the LPO pathway, strikingly inhibited by allopurinol. Although allopurinol inhibited XO activity in cell-free extract (<97%), PEG had no effect at all. In multiple evaluations of the mechanisms of PEG reduction of ROS and the products of LPO, it is thus clear that the polymer does not do this by direct action as a scavenger or an inhibitor (Luo et al., 2002; Luo, Shi, and Borgens, unpublished observations).

In summary, P188 may be a free radical scavenger (Marks et al., 2001), whereas PEG is not. They both, however, directly reduce ROS and LPO in the damaged nervous system. Furthermore, they both provide neuroprotection to injured spinal cord and thus will continue to be investigated as a potential therapies, simple to apply, for various forms of neurotrauma.

ACKNOWLEDGMENTS

This work was supported by grants from the National Institutes of Health (1 RO1 NS 39288-01 and 1 RO1 NS/HD 39288-01A1 to R.B.B., R01 GM61101 and R01 GM64757 to R.C.L.). We thank the State of Indiana for financial support of the Center for Paralysis Research, Mrs. M. Hulman George and H. Skinner for generous gifts, and the Intel Corporation for their generous support through gifts of advanced computer hardware. We also thank A. Altizer for expert assistance, K. Harrington for artwork, and S. Folyer for manuscript production.

REFERENCES

Bajaj CL, Pascucci V, Schikore DR. 1997. The contour spectrum. In: Yagel R, Hagen H, editors. Proceedings of the IEEE Visualization 1997 Conference. Phoenix, Arizona: IEEE Computer Society Press. p 167–175.

Bindokas VP, Jordan J, Lee CC, Miller RJ. 1996. Superoxide production in rat hippocampal neurons: selective imaging with hydroethidine. J Neurosci 16:1324–1336.

Blight AR. 1991. Morphometric analysis of a model of spinal cord injury in guinea pigs, with behavioral evidence of delayed secondary pathology. J Neurol Sci 103:156–171.

Blight AR, McGinnis ME, Borgens RB. 1990. Cutaneus trunci muscle reflex of the guinea pig. J Comp Neurol 296:614–633.

Borgens RB. 1982. What is the role of naturally produced electric current in vertebrate regeneration and healing? Int Rev Cytol 76:245–298.

Borgens RB. 1992. Applied voltages in spinal cord reconstruction: history, strategies, and behavioral models. In: Illis LS, editor. Spinal cord dysfunction, Vol III. Functional stimulation. Oxford: Oxford Medical Publications. p 110–145.

Borgens RB. 2001. Cellular engineering: molecular repair of membranes to rescue cells of the damaged nervous system. Neurosurgery 49:370–379.

Borgens RB. 2003. Restoring function to the injured human spinal cord. Heidelberg: Springer-Verlag. 161 p.

Borgens RB, Blight AR, McGinnis M. 1987. Behavioral recovery induced by applied electric fields after spinal cord hemisection in guinea pig. Science 238:366–369.

Borgens RB, Blight AR, McGinnis ME. 1990. Functional recovery after spinal cord hemisection in guinea pigs: the effects of applied electric fields. J Comp Neurol 296:634–653.

Borgens RB, Bohnert DM. 2001. Rapid recovery from spinal cord injury after subcutaneously administered polyethylene glycol. J Neurosci Res 66:1179–1186.

Borgens RB, Shi R. 2000. Immediate recovery from spinal cord injury through molecular repair of nerve membranes with polyethylene glycol. FASEB 14:27–35.

Borgens RB, Shi R, Bohnert D. 2002. Behavioral recovery from spinal cord injury following delayed application of polyethylene glycol. J Exp Biol 205:1–12.

Chan PH, Kawase M, Murakami K, Chen SF, Li Y, Calagui B, Reola L, Carlson E, Epstein CJ. 1998. Overexpression of SOD1 in transgenic rats protects vulnerable neurons against ischemic damage after global cerebral ischemia and reperfusion. J Neurosci 18:8292–8299.

Donaldson J, Shi R, Borgens R. 2002. Polyethylene glycol rapidly restores physiological functions in damaged sciatic nerves of guinea pigs. Neurosurgery 50:147–157.

Duerstock BS, Bajaj CL, Pascucci V, Schikore D, Lin KN, Borgens RB. 2000. Advances in three-dimensional reconstructions of the experimental spinal cord injury. Comput Med Imag Graph 24:389–406.

Duerstock BS, Borgens RB. 2002. Three-dimensional morphometry of spinal cord injury following polyethylene glycol treatment. J Exp Biol 205:13–24.

Follis F, Jenson B, Blisard K, Hall E, Wong R, Kessler R, Temes T, Wernly J. 1996. Role of poloxamer 188 during recovery from ischemic spinal cord injury: a preliminary study. J Invest Surg 9:149–156.

Hall ED 1992. The neuroprotective pharmacology of methylprednisolone. J Neurosurg 76:13–22.

Hannig J, Zhang D, Canaday DJ, Beckett MA, Astumian RD, Weichselbaum RR, Lee RC. 2000. Surfactant sealing of membranes permeabilized by ionizing radiation. Radiat Res 154:171–177.

Koh JY, Choi DW. 1987. Quantitative determination of glutamate mediated cortical neuronal injury in cell culture by lactate dehydrogenase efflux assay. J Neurosci Methods 20:83–90.

Lee J, Lentz BR. 1997. Evolution of lipid structures during model membrane fusion and the relation of this process to cell membrane fusion. Biochem 36:6251–6259.

Lee RC, Myerov A, Maloney CP. 1994. Promising therapy for cell membrane damage. Ann N Y Acad Sci 720:239–245.

Lee R, River LP, Pan FS, Ji L, Wollmann RL. 1992. Surfactant-induced sealing of electropermeabilized skeletal muscle membranes in vivo. Proc Natl Acad Sci USA 89:4524–4528.

Leskovar A, Moriarty LJ, Turek J, Schoenlein IA, Borgens RB. 2000. The macrophage in acute neural injury: changes in cell numbers over time and levels of cytokine production in mammalian central and peripheral nervous systems. J Exp Biol 203:1783–1795.

Lewen A, Matz P, Chan PH. 2000. Free radical pathways in CNS injury. J Neurotrauma 17:871–890.

Luo J, Borgens RB, Shi R. 2002. Polyethylene glycol immediately repairs neuronal membranes and inhibits free radical production after acute spinal cord injury. J Neurochem 83:1–10.

Marks JD, Pan CY, Bushell T, Cromie W, Lee RC 2001. Amphiphilic, tri-block copolymers provide potent, membrane-targeted neuroprotection. FASEB 15:1107–1109.

Maskarinec SA, Hannig J, Lee RC, Lee KY. 2002. Direct observation of Poloxamer 188 insertion into lipid monolayers. Biophys J 82:1453–1459.

Mellors A, Tappel AL. 1966. The inhibition of mitochondrial peroxidation by ubiquinone and ubiquinol. J Biol Chem 241:4353–4356.

Merchant FA, Holmes WH, Capelli-Schellpfeffer BS, Lee RC, Toner M. 1998. Poloxamer 188 enhances functional recovery of lethally heat-shocked fibroblasts. J Surg Res 74:131–140.

Moriarty LJ, Borgens RB 1999. The effect of an applied electrical field on macrophage accumulation within the subacute spinal injury. Rest Neurol Neurosci 14:53–64.

Moriarty LJ, Duerstock BS, Bajaj CL, Lin K, Borgens RB. 1998. Two and three dimensional computer graphic evaluation of the subacute spinal cord injury. J Neurol Sci 155:121–137.

Padanlam JT, Bischof JC, Cravalho EG, Tompkins RG, Yarmush ML, Toner M. 1994. Effectiveness of Poloxamer 188 in arresting calcein leakage from thermally damaged isolated skeletal muscle cells. Ann N Y Acad Sci 92:111–123.

Palmer JS, Cromie WJ, Lee RC. 1998. Surfactant administration reduces testicular ischemia-reperfusion injury. J Urol 159:2136–2139.

Quick KL, Hardt JI, Dugan LL. 2000. Rapid microplate assay for superoxide scavenging efficiency. J Neurosci Methods 97:139–144

Shi R, Borgens RB. 2000. Anatomical repair of nerve membranes in crushed mammalian spinal cord with polyethylene glycol. J Neurocytology 29:633–644.

Shi R, Borgens RB, Blight AR. 1999. Functional reconnection of severed mammalian spinal cord axons with polyethylene glycol. J Neurotrauma 16:727–738.

Shi R, Asano T, Wining NC, Blight AR. 2000. Control of membrane sealing in injured mammalian spinal cord axons. J Neurophysiol 84:1763–1769.

Terry MA, Hannig J, Carrillo CS, Beckett MA, Weichselbaum RR, Lee RC. 1999. Oxidative cell membrane alteration: evidence for surfactant-mediated sealing. Ann N Y Acad Sci 888:274–284.

Tuszynski MH, Gabriel K, Gerhardt K, Szollar S. 1999. Human spinal cord retains substantial structural mass in chronic stages after injury. J Neurotrauma 16:523–531.

Young W. 1993. Secondary injury mechanisms in acute spinal cord injury. J Emerg Med 11:13–22.